Electron Density Distribution near Large Air Shower Axes at Sea Level*†

R. E. Heineman‡
H. M. Randall Laboratory, University of Michigan, Ann Arbor, Michigan
(Received April 15, 1954)

A large, multiple-wire ionization chamber has been used to sample 20 separate areas of the plane of observation to obtain detailed "profiles" of the structure of large air showers within about 2 meters of their axes. Interpretation of the data is based on (1) quantitative calculations of the transition effect in 0.305 radiation lengths of dural, and (2) a semiquantitative discussion of the fluctuations in the lateral-distribution function. Lateral distribution functions for electrons and photons of various energies have been calculated for $r < 10$ meters at the shower maximum and the function for electrons of all energies turns out to be essentially equal to the one given by Molière. No drastic revision of the calculated distribution function is indicated by the data, but a flatter distribution than that calculated is not ruled out. Evidence for a multiple-core structure in a small percentage of cases is presented.

I. INTRODUCTION

IT has been supposed[1] for some time that a neutral π meson, the π^0, which decays into two photons after a very short lifetime, initiates the high-energy electronic cascades commonly called large air showers. This belief grew stronger as the existence of the π^0 was confirmed in the laboratory[2] and as experimental evidence was obtained in cloud-chamber work[3–5] which showed that π^0 mesons are the main, if not the exclusive, source of photons associated with cosmic-ray nuclear events. If a cascade shower is produced from each high-energy photon created in the decay of an energetic π^0 meson, and if there is a multiplicity of π^0's similar to the multiplicity of charged π mesons produced in high-energy nuclear events,[6] then it would be expected that, in general, large air showers would be composed of multiple shower cores. The lack of experimental confirmation of such multiple-cored events does not disprove the suspected π^0-meson origin since the numbers of such particles produced, their angular distribution, and their energy distribution are probably not known.[7] It seemed, therefore, that a more detailed study of the electron density in *individual* high-energy events than had been performed[8,9] previously might

produce evidence as to their origin and shed some light on the characteristics of π^0 production.

At the time the work to be described here[10] was begun it could only be stated that the available data[8,9] on the electron-density distribution in large air showers at distances from 2 to 100 meters from the core gave no indication of a multiple-core structure, and, moreover, showed no incompatibility with the theoretical distribution obtained by Molière[11] for a single shower core. More recent studies[12,13] of the electron distributions found by using a large cloud chamber or a cloud chamber in conjunction with five ionization chambers presented evidence of a "lumpy" distribution near the axes of the showers in a small percentage of cases. The experimental shower "profiles" to be presented here (some of which appeared in reference 10) are in substantial agreement with the foregoing conclusion.

The present experiment was designed to obtain the electron-density distribution within 2 meters of the core in each useful shower event recorded by using a multiple-wire ionization chamber. The chamber has a sensitive area of 0.97 m² and a wire separation of 10 cm for each of the 20 pulse channels. The use of such a chamber combines the well-defined density measurement obtainable with an ion chamber (as compared to geiger-counter arrays) with the resolution of a cloud chamber. This apparatus is capable of resolving two cores, each having equal energies and "$1/r$" density distributions, separated by 30 to 60 cm in a direction perpendicular to the chamber wires. The actual resolution is dependent upon the local size of the shower and the distance of the axes from the center of the chamber.

The data were obtained at an elevation of about 280 meters and, therefore, at a depth in the atmosphere 26.4-radiation lengths where the characteristic scatter-

* Supported in part by the U. S. Office of Naval Research and the U. S. Atomic Energy Commission.
† Based on a thesis submitted in partial fulfillment of the requirements for a Ph.D. degree at the University of Michigan, Ann Arbor, Michigan.
‡ Present address: General Electric Company, Hanford Atomic Products Operation, Richland, Washington.
[1] Lewis, Oppenheimer, and Wouthuysen, Phys. Rev. 73, 127 (1948).
[2] Bjorklund, Crandall, Moyer, and York, Phys. Rev. 77, 213 (1950); Panofsky, Aamodt, Hadley, and Phillips, Phys. Rev. 80, 94 (1950); Steinberger, Panofsky, and Steller, Phys. Rev. 78, 802 (1950).
[3] B. Gregory and J. Tinlot, Phys. Rev. 81, 675 (1951).
[4] P. R. Barker, Phys. Rev. 81, 291 (1951).
[5] G. Salvini and Y. B. Kim, Phys. Rev. 88, 40 (1952).
[6] Kaplan, Ritson, and Walker, Phys. Rev. 90, 716 (1953); Lal, Pal, Peters, and Swami, Proc. Indian Acad. Sci. 36, 75 (1952); Lord, Fainberg, and Schein, Phys. Rev. 80, 970 (1950); see also, E. Fermi, Progr. Theoret. Phys. 5, 570 (1950).
[7] Hazen, Heineman, and Lennox, Phys. Rev. 86, 198 (1952).
[8] R. W. Williams, Phys. Rev. 74, 1689 (1948).
[9] Cocconi, Tongiorgi, and Greisen, Phys. Rev. 76, 1020 (1949).

[10] Some of the work and results contained here have been briefly outlined previously: R. E. Heineman and W. E. Hazen, Phys. Rev. 90, 496 (1953).
[11] G. Molière, Cosmic Radiation (Dover Publications, New York, 1946).
[12] W. E. Hazen, Phys. Rev. 85, 455 (1952).
[13] Hazen, Williams, and Randall, Phys. Rev. 93, 578 (1954).

ing length r_1 is 80 m. We have used $X_0 = 37.7$ g/cm^2 for the radiation length in air. The sensitive volume of the chamber was shielded from the upper hemisphere by the chamber cover plate of 1-in. dural and an additional 0.05 in. of aluminum. The transition effect in this material is calculated in Sec. III. The chamber was placed with its long axis in a north-south direction, which thus minimizes the effect (only recently pointed out by Cocconi[14]) of the earth's magnetic field on the electron lateral distribution.

II. EXPERIMENTAL

A. General

A block diagram of the equipment used is presented in Fig. 1.

When all 4 Geiger counters are discharged within the resolving time (45 μsec) of the coincidence circuit, the probability is great that a shower core has hit within a few meters of the center of the ionization chamber. The output of the coincidence circuit trips the sweep and brightener circuits of a 20-channel synchroscope which displays the amplified pulses from the ion chamber. The electron pulses induced on the central wires of the chamber by the passage of shower electrons through the chamber are separately amplified, first by preamps having a clipping time constant of about 700 μsec, and then by a 20-channel amplifier. The latter amplifier was purposely constructed to be moderately nonlinear to accommodate a larger range of input voltage pulses. After the array of pulses appearing on the cathode-ray tubes are recorded on 35-mm film, a trigger from the synchroscope rewinds the camera in preparation for the next 4-fold coincidence and records a count on a mechanical register. The time of each event is also recorded by briefly illuminating the face of a clock mounted on the synchroscope chassis. The long time constants in the amplifiers are necessary because of the poor photographic properties of the light output from the green-phosphor cathode-ray tubes used. The Geiger counters have a sensitive area of 350 cm^2 and were positioned at the ends and sides of the ionization chamber, 132 and 67 cm from the center of
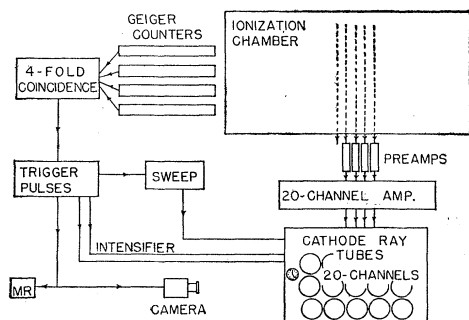

FIG. 1. Block diagram of experimental apparatus.

[14] G. Cocconi, Phys. Rev. 93, 646 (1954).

the chamber, respectively. Since the selection of interesting events can easily be made by looking at the photographic record, a more selective triggering system is not necessary.

B. Ionization Chamber

The ionization chamber, shown schematically in Fig. 2 with the top plate removed, has $\frac{5}{16}$-in. steel sides, 1-in. dural top and bottom, and has a collecting volume of 7 ft 6 in. $\times$ 25 in. $\times$ 8 in. To make end effects small (transition effect in the steel walls and capacitance to the end walls), a dummy collecting wire is placed at each end of the chamber. Grounded cylindrical guard rings are used on both ends of each of the remaining 20 collecting wires which are connected to the ground through separate 100-meg resistors. The chamber itself is connected to the high-voltage supply and shielded by a grounded aluminum and galvanized-iron box.

Calibration polonium-α sources were deposited on a copper rod which lies inside a brass cylinder on the bottom of the chamber. The rod can be turned so that α particles are emitted through holes in the cylinder beneath each of the 20 wires or turned so that they are completely absorbed in the walls of the cylinder. In addition, one source is so constructed that it can be moved vertically from the bottom plate up to the wire above it in order to test for electron attachment in impurities in the argon filling the chamber. This test
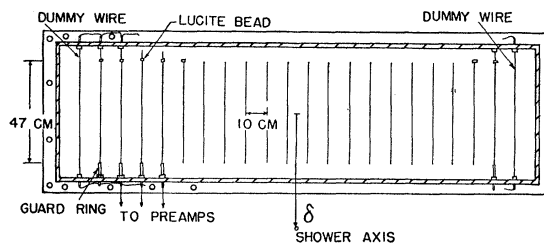

FIG. 2. Schematic diagram of the ion chamber with its 1-in. dural top removed. The parameter δ locates the shower axis in a direction perpendicular to the long axis of the chamber.

was suggested by Driggers,[15] and his results are confirmed as described below.

The α-pulse heights which were recorded as the movable source was positioned at varying distances from the central wire, before and after successive attempts at purification of the argon, are shown in Fig. 3. The argon was purified by circulating it through a heated cylinder containing calcium turnings. Positive circulation was ensured by connecting a centrifugal fan to the rotor of an induction motor within the pressurized system. For the case in which there is no attachment the α-pulse heights should decrease as the source is moved closer to the wire, because of the ionization being deposited in regions of lower potential. This

[15] F. E. Driggers, Phys. Rev. 87, 1080 (1952).

decrease should not be very drastic since the range of the α particles is only 0.5 cm (37 psia of argon) and the rod is in contact with the high voltage shell of the chamber. To predict the decrease quantitatively is difficult since the field geometry is complicated and the source emits particles in any direction within the upper hemisphere. For the latter reason, it is expected that widely varying pulse heights should be observed for source-to-wire distances that are of the order of the range of the alpha particles. This was indeed observed and makes the uncertainty in the pulse-height determinations relatively large for these small distances. The decrease in pulse height from curve I to II is assumed to be caused by outgassing of the calcium turnings and
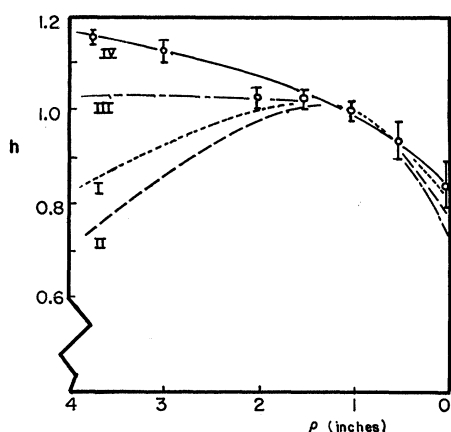

FIG. 4. Saturation curves taken with an α source at the bottom of the chamber before (I) and after (II) purification of the argon: α-pulse height h vs chamber voltage U_0.

FIG. 3. Relative polonium α-pulse height h vs distance ρ of an α source from a central collecting wire. The curves are normalized to 1.0 at $\rho = 1$. The data in curve I were taken before attempting purification, and the data for the other curves were taken after the purifier had been operated for 4 hours at 250 watts (II), 2 hours at 500 watts (III), and 3 hours at 500 watts (IV). Typical estimated errors are given for curve IV.

purifier, while curves III and IV indicate a decreasing attachment probability with further purification.

In Fig. 4 are presented typical saturation curves of a single channel taken before and after purification. They show the α-pulse height for a stationary source vs the chamber high-voltage. From the shapes of these curves it is evident that the saturation of the α-pulse height as the chamber voltage is increased does not necessarily, in itself, indicate the absence of electron attachment.

C. Measurement of Ionization

The passage of a high-energy shower electron through the chamber produces ionization, low-energy electrons, and positive argon ions. The quantities measured directly for each event are the numbers of these secondary electrons which are liberated within the sensitive volumes of each of the 20 wires, as described in this section. It will be shown in the next section that there is a simple relationship between these
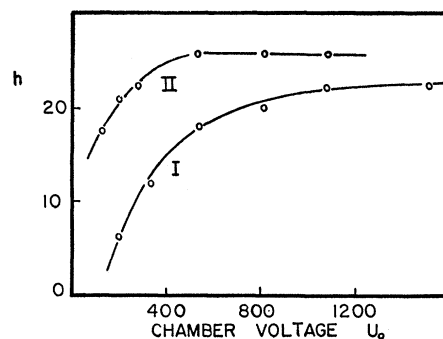
numbers and the numbers of shower electrons passing through each of these volumes.

Rossi and Staub[16] have shown that the voltage pulse appearing across the collecting electrode and ground of an ion chamber is

$$V = \frac{e}{C} \frac{1}{U} \sum_{i=1}^{N_0} U_i,$$

if the output-time constant of the chamber is so long that all the electrons are collected but short enough so that the positive ions have not moved appreciably from their position of formation when the pulse begins to decay. In this expression, C is the output capacitance of the collecting electrode, e is the charge on an electron, U is the high voltage on the chamber, N_0 is the number of ion pairs formed in the sensitive volume of the collecting electrode, and U_i is the potential at the position of formation of the ith ion pair. Since the number of shower electrons passing through the chamber in each recorded event will be rather large, it is reasonable to assume that little error will be incurred by using the value of $\sum_i U_i$ which would be found for a uniform distribution of ionization throughout each sensitive volume. Then we may write

$$V = \frac{eN_0}{C} \frac{\bar{U}_i}{U} = \frac{eN_0}{C} f,$$

where $f = 0.87$, as calculated for our chamber geometry. It can easily be shown that the presence of one dummy wire on each end of the chamber is sufficient to make the value of f essentially the same for all collecting volumes.

It is obvious that the foregoing method of finding the voltage pulse on a wire may be validly applied to our chamber only insofar as the ionization which is collected solely on that wire does not affect the potentials of the other wires. The magnitude of the

[16] B. Rossi and H. Staub, *Ionization Chambers and Counters* (McGraw-Hill Book Company, Inc., New York, 1949).

induction effect has been calculated[17] for the case in which there is a uniform density of ionization throughout the collecting volume of one wire, whose voltage is thereby changed by an amount V. Then it was found that the voltage V_1 on an immediately adjacent wire is given by $V_1 = -0.027V$. The effect is so small that it is neglected.

D. Calibration

Since the energy loss by ionization for relativistic electrons is almost independent of their energy, it can be assumed that each shower electron, in passing through the chamber of height l centimeters, liberates the same number of ion pairs $N_0 = lj\delta$. δ is the density of argon in g/cm³ and j is the average specific ionization of the electron in ion pairs per g/cm². Then, from the previous section the voltage pulse produced by Π shower electrons whose ionization is all collected on one wire is given by

$$V = \Pi N_0 ef/C = \Pi eflj\delta/C.$$

To calibrate the output voltage V, either a known amount of ionization must be placed in the chamber or the capacitance C determined. Since C is very difficult to evaluate, the former method is used. It has been shown[18] that the number of ion pairs formed by an alpha particle in argon is proportional to its energy. If we let W_0 be the energy necessary to form one ion pair, the pulse height V_α observed because of the collection of the charge produced by an alpha particle of energy E_α is $Q_\alpha/C = (E_\alpha/W_0)/C$. The factor f does not appear because the α sources are located near the shell of the chamber where the potential changes only slightly within a distance equal to the range of the α particles. Eliminating the capacitance in the above expressions, we find

$$\Pi = \frac{E_\alpha}{eflj\delta jW_0} \frac{V}{V_\alpha}.$$

Since it is believed[19] on theoretical grounds that the energy W_0 expended to form one ion pair is independent of the type of ionizing particle, jW_0 may be considered to be the energy dissipated in collision processes by the shower electron. Since the average energy of shower electrons is 100 Mev,[20] jW_0 is found to be 2.1×10^6 ev g/cm². It is to be noted that the *total* energy loss by collision should be used since shower theory, which is used to interpret the data, does not count energetic secondary electrons produced by collision as separate shower electrons. Though some collisions give rise to

secondary electrons so energetic that they do not dissipate all their energy before leaving the argon, there are a compensating number of secondary electrons entering the chamber since the collision probabilities and energy loss in argon and in air (or aluminum) are almost the same.

Calibration pulses are recorded by uncovering the sources and tripping the sweep circuit at random. Since the alphas are released at random also, the superposition of a large number of sweeps produces a row of pulses whose heights can easily be measured. As a secondary calibration for the nonlinear amplifiers, a precision pulser is used to pulse the shell of the chamber, inducing pulses of identical voltages on all 20 channels, and to trip the sweep circuit simultaneously.

By comparing an α pulse with the induced-pulse heights the capacitance C can be calculated. Using a value[15] of 26.4 ev for W_0, we find that $C = 4.2$ $\mu\mu$f. A value calculated from the geometry of the chamber is 4.3 $\mu\mu$f. Considering the difficult geometry and the uncertainty in W_0, we find the agreement better than could be expected. This calculation is of interest because it increases our faith in the similar calculations of the induction effect between channels.

III. THEORETICAL CONSIDERATIONS

It was shown in section II that the pulse heights on the cathode-ray tubes could be interpreted in terms of numbers of electrons traversing the sensitive volumes of the ionization-chamber wires. However, because of the transition effect in the 1.05 in. of dural above the collecting volume of the chamber, these numbers are not necessarily the same as the numbers of electrons in the air shower incident on the dural. Since this effect is dependent upon the energies and the relative numbers of electrons and photons, it depends also upon r, distance from the shower axis. Therefore, in part A below we use the results of shower theory to calculate the lateral distribution of electrons under 1.05-in. dural, and from this distribution we calculate, in B, the response of the ion-chamber channels to such a distribution. We must then look for consistency between observed data and the calculated response curves. If inconsistencies are found, they could conceivably be explained by assuming that (1) shower theory, as used here, inadequately describes the showers observed; (2) there is a multiplicity of cores associated with a particular event; or (3) the fluctuations in the lateral development of showers are large. These possible departures from the response curves calculated for the average single shower core are discussed in C and D.

A. Lateral Distribution of Electrons Under 1.05 in. Dural

A general description of the method used to find this distribution will first be given. The calculations of the

[17] R. E. Heineman, thesis, University of Michigan, 1953 (unpublished).
[18] Jesse, Forstat, and Sadauskis, Phys. Rev. 77, 782 (1950).
[19] B. Rossi, *High Energy Particles* (Prentice-Hall, Inc., New York, 1952).
[20] B. Rossi and K. Greisen, Revs. Modern Phys. 13, 240 (1941).

specific functions and constants required by this method are outlined in the succeeding subsections.

Let $P_r(E,r,s)rdrdE$ be the average relative number of electrons of energy E in dE passing through the plane of observation in an annular ring between r and $r+dr$ from the axis, and in a direction making any angle ϑ with the axis, of a shower of age s. Let this function be normalized such that

$$\int_0^\infty P_r(E,r,s)rdr = \frac{\pi(E_0,E,t)}{\Pi(E_0,0,t)},$$

and (1)

$$\int_0^\infty \int_0^\infty P_r(E,r,s)rdrdE = 1,$$

where $\pi(E_0,E,t)dE$ is the number of electrons of energy E in dE found at a depth t from the origin of a shower of total energy E_0 and $\Pi(E_0,0,t)$ is the number of electrons in the shower at depth t having energies $E>0$. The age parameter s is a function of E_0 and t, defined by Eq. (2.104) of reference 19. Let $Q_r(W,r,s)rdrdW$ be a similar function for the photons of energy W, where

$$\int_0^\infty Q_r(W,r,s)rdr = \frac{\gamma(E_0,W,t)}{\Pi(E_0,0,t)},$$ (2)

and γ is the differential photon spectrum. Q_r is normalized with respect to Π because, in the usual shower theory approximations, the corresponding integral photon function, $\lim_{W\to 0}\Gamma(E_0,W,t)$, is infinite.

Let $\mathfrak{N}(E_1,E_2;r,s,\tau)$ be the relative number of electrons of energy between E_1 and E_2 found in an annular ring between r and $r+dr$ under a thickness of absorber τ when a shower of age s is incident above the absorber; and let $n(E',r,s,\tau)dE'$ be the corresponding number of electrons of energy E' in dE'. Then we may write

$$\mathfrak{N}(E_1,E_2;r,s,\tau) = \int_{E_1}^{E_2} n(E',r,s,\tau)dE,$$

and (3)

$$n(E',r,s,\tau) = \int_0^\infty T(E,E',\tau)rP_r(E,r,s)dE$$
$$+ \int_0^\infty T(W,E',\tau)rQ_r(W,r,s)dW.$$

The function $T(E,E',\tau)$ is the number of electrons of energy E' created in the absorber, relative to the number of electrons of energy E which were incident on the absorber and led to their creation. Similarly, $T(W,E',\tau)$ is the number of electrons of energy E' produced relative to the number of incident photons of energy W which led to their creation. It is assumed that neither a particle nor any of its secondary electrons experiences a displacement in r in traversing the layer. For the great majority of all electrons, this displacement

is small compared to the separation of the detector areas in this experiment.

The function we want to calculate, $\mathfrak{N}(0,\infty;r,s,\tau)$, for τ equal to 1.05-in. dural, or $0.304X_0$, is normalized such that

$$\int_0^\infty \mathfrak{N}(0,\infty;r,s,\tau)dr = \frac{\Pi(E_0,0,t+\tau)}{\Pi(E_0,0,t)}.$$

The dependence of $\mathfrak{N}$ on τ will not be shown hereafter since we shall be interested in only one value of this parameter. Because very little is known about P_r and Q_r for any point in the shower development except the maximum, it will be assumed that all showers incident on the chamber are at their maximum. The dependence on s need not be shown explicitly since $s=1$ will be understood.

The integrations in (3) must be performed numerically since good analytical functions for P_r and Q_r are not available for all energies. The functions $T(E,E')$ and $T(W,E')$ vary slowly with E and W. We may therefore use a small number of energy intervals ΔE_i and ΔW_i and represent the functions T in each interval by constants, which are called *transition factors*. They are the values of the functions calculated at an energy equal to the median electron energy of each interval. With the above simplications, we use (3) and obtain

$$\mathfrak{N}(0,\infty;r) = \sum_j n(\Delta E_j;r),$$

and (4)

$$n(\Delta E_j,r) = \sum_i \{T(\bar{E}_i,\Delta E_j)N_e(\Delta E_i;r)$$
$$+ T(\bar{W}_i,\Delta E_j)N_p(\Delta W_i;r)\},$$

where

$$N_e(\Delta E_i;r) = \int_{\Delta E_i} rP_r(E,r)dE$$ (5)

is the distribution function for incident electrons having energies in the energy range ΔE_i. $N_p(\Delta E_i;r)$ is a similar function for the incident photons. Equation (4) may be rewritten, so that the distribution function for electrons of all energies under the layer of dural is

$$\mathfrak{N}(0,\infty;r) = \sum_i \{\sum_j [T(\bar{E}_i,\Delta E_j)]N_e(\Delta E_i;r)$$
$$+ \sum_j [T(\bar{W}_i,\Delta E_j)]N_p(\Delta W_i;r)\}. \quad (6)$$

(1) Lateral Distributions of Incident Electrons—$N_e(E_1,E_2;r)$

The incident electrons have been divided into five energy ranges, and the corresponding radial distribution functions which have been calculated are shown in Fig. 5.

From Eqs. (1) and (5), it is seen that these functions must satisfy the condition that

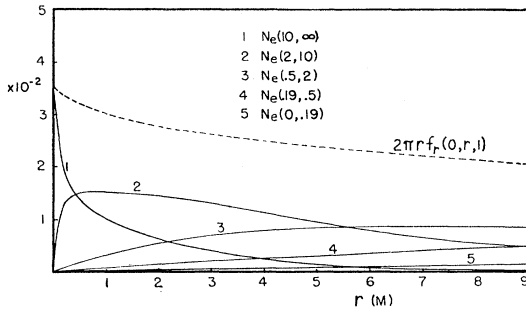$$\int_0^\infty N_e(E_1,E_2;r)dr \cong \frac{P_0(E_0,E_2)-P_0(E_0,E_1)}{P_0(E_0,0)}, \quad (7)$$

FIG. 5. Lateral distribution functions for shower electrons of energy in the range ΔE_i, $N_e(E_1,E_2;r)$, and the Molière function, $2\pi r f_r$, for electrons of all energies. The curves refer to showers at their maximum in air where $r_1 = 80$ m. Energies are in units of the critical energy ϵ_0.

where $P_0(E_0,E)$ is the integral track length of electrons of energy greater than E, used in shower theory.[19,20] The approximation indicated is best when E_0 and t are such that the shower is at its maximum. To evaluate (7) we have connected the numerical results of Richards and Nordheim,[21] for $E \leq 3\epsilon_0$, to the results of shower theory Approximation A, where ϵ_0 is the critical energy in air, 84.2 Mev.[19] These results allow a normalization of the functions $P_r(x)$, where $x = (Er)/\epsilon_0 r_1$, given by Eyges and Fernbach.[22]

Since the method used by EF did not give the behavior of the functions $P_r(x)$ near $x = 0$, they did not prescribe their functions in this region except for very high energies, $E > 10\epsilon_0$. In this case they used the similar high-energy function obtained by Molière to continue their function to $x = 0$. Since the Molière function does not fit smoothly with the distributions given by EF for lower energies, we have continued the latter to zero (on a log-log plot in which the curvature is minimized) in such a way that they preserve the general shape of Molière's high-energy function. It is to be noted, however, that the normalization is found independently and that there is little freedom left in the process of continuing the curves smoothly to zero.

It is perhaps surprising that the sum of our distribution functions is essentially equal to the total-distribution function of Molière[11] since different approximations have been used in each. The form of this function which has been given by Bethe[8] is

$$2\pi r f_r(0,r,1) = 0.454(2\pi r_1)(1+4r/r_1)\exp[-4(r/r_1)^{\frac{2}{3}}],$$

and is shown in Fig. 5 also. Actually, we might hope that our treatment is better than that of Molière for the range of r considered. For high energies, $E > 10\epsilon_0$, the functions used here are probably better, though equal to Molière's high-energy function near $r = 0$. For intermediate energies, $2\epsilon_0 \leq E \leq 10\epsilon_0$, the functions used are similar to Molière's high-energy function for $r < 10$

m, but differ in their normalization. For low energies, $E < 2\epsilon_0$, the function used was that constructed from the EF function for $E = 2\epsilon_0$. Though this function would again be similar to the one used by Molière, the relative numbers of low-energy electrons should be quite reliable in our calculations as compared with the rather poor approximations available to Molière (see Blatt[23]). Though there has been some controversy recently[24,25] concerning the assumptions underlying the calculations of EF and Molière, our use of the results of the former can be regarded as a choice of a first-order approximation which seems to have given at least fair agreement with experiment in the past.

(2) Lateral Distributions of Incident Photons—$N_p(W_1,W_2;r)$

The calculated lateral photon distributions for the four ranges of photon energies above $0.19\epsilon_0$ are shown in Fig. 6, together with Molière's electron distribution for $E > 0$ (dotted). The photon distributions were obtained as follows.

A comparison of the renormalized Molière photon distribution,[26] for energies $W \gg \epsilon_0$, with the numerical photon distributions, for energies $W > 10\epsilon_0$ and $W = 10\epsilon_0$, $5\epsilon_0$, and $2\epsilon_0$, given by Eyges and Fernbach,[22] showed good agreement for the range of r to be considered. The renormalized,[22] analytical distribution $Q_r'(x)$ of Molière was therefore used, since it could be integrated easily. This distribution is

$$Q_r'(x) = \frac{31.94 \exp\left(-\dfrac{2x}{(0.1)^{\frac{1}{2}}}\right)}{\dfrac{2x}{(0.1)^{\frac{1}{2}}}} + \frac{0.806}{3.25}\exp\left(-\frac{2x}{(3.25)^{\frac{1}{2}}}\right)$$

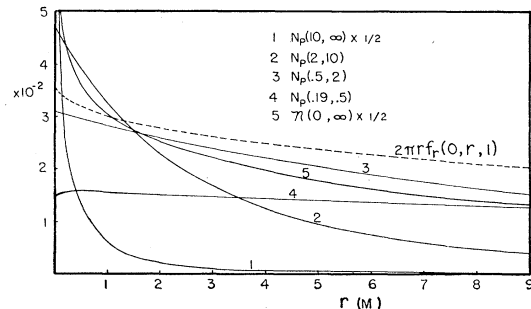where $x = (Wr)/\epsilon_0 r_1$ and $\int_0^\infty Q_r'(x)x\,dx = 1$. This function

FIG. 6. Lateral distribution functions for shower photons of energy in the range ΔW_i, $N_p(W_1,W_2;r)$; the Molière electron distribution, $2\pi r f_r$; and the distribution function for electrons of all energies under 1.05-in. dural, $\mathfrak{N}(0,\infty;r)$. The curves refer to showers at their maximum in air where $r_1 = 80$ m. Energies are in units of the critical energy ϵ_0.

[21] J. Richards and L. Nordheim, Phys. Rev. 74, 1106 (1948).
[22] L. Eyges and S. Fernbach, Phys. Rev. 82, 23 (1951), hereinafter referred to as EF.

[23] J. M. Blatt, Phys. Rev. 75, 1584 (1949).
[24] H. S. Green and H. Messel, Phys. Rev. 88, 331 (1952).
[25] G. Molière, Phys. Rev. 93, 636 (1954).
[26] G. Molière, Phys. Rev. 77, 715 (1950).

is normalized correctly for high energies where the Approximation A of shower theory is correct. Since it does not give the correct numbers of photons at lower energies, we introduce a correction function $\sigma(W)$ given by

$$\sigma(W) = \frac{r_1^2}{0.437} \frac{Q_r(W,r)}{Q_r'(x)}.$$

By comparing the normalization of $Q_r'(x)$ with that for $Q_r(W,r)$ given by (2), we find

$$\sigma(W) = \frac{1}{0.437} \left(\frac{W}{\epsilon_0}\right)^2 \frac{\gamma(E_0,W,t)}{\pi(E_0,W,t)} \frac{\pi(E_0,W,t)}{\Pi(E_0,0,t)},$$

from which $\sigma(W)$ will be calculated. At high energies under Approximation A, it is found that $\gamma/\pi = 9/7$ and $\pi/\Pi = 0.437(\epsilon_0/W)^2$. At lower energies we equate γ/π to $g_0(E_0,W)/p_0(E_0,W)$, where g_0 and p_0 are the differential track lengths of photons and electrons of energy W, respectively; and π/Π to $p_0(E_0,W)/P_0(E_0,0)$, where $P_0(W,0)$ is the integral track length of all electrons having energy $W > 0$. Using values for the track lengths calculated by Richards and Nordheim,[21] we plot g_0/p_0 as curve I and $(\pi/\Pi)_{\text{Approx A}}/(p_0/P_0)$ as curve II in Fig. 7. It is seen that both curves vary much more rapidly with energy than $1/\sigma(W)$, shown as curve III in Fig. 7.

The incident photon distributions can then be written

$$N_p(W_1,W_2;\,r) = \frac{0.437}{r_1^2}\sigma(\overline{W}_i)\int_{x_1}^{x_2} Q_r'(x)dx, \qquad (8)$$

where $\sigma(W)$ has been replaced by an average value, $\sigma(\overline{W}_i)$, over the energy range considered. The values of $\sigma(\overline{W}_i)$ which were used are given in Table I.

In calculating the distribution for the highest energy range, $(10\epsilon_0,\infty)$, W_2 in (8) should not, of course, be ∞, but some upper limit $W_{\text{max}} < E_0$. Even though the lower limit, W_1, is much less than W_{max} in our case, the detailed behavior of the integral for r less than 5 or perhaps 10 cm is dependent upon W_{max}. Since our ionization chamber is insensitive to changes in the distribution function at such small distances from the shower core, we have made suitable assumptions concerning the height of production of the showers, their energies, and the degradation of this energy. The approximations made should give an adequate representation of the distribution near $r=0$ for all showers observed.

TABLE I. The average values of $\sigma(W)$, $\sigma(\overline{W}_i)$, for the energy ranges (W_1,W_2). Energies are in units of the critical energy ϵ_0.

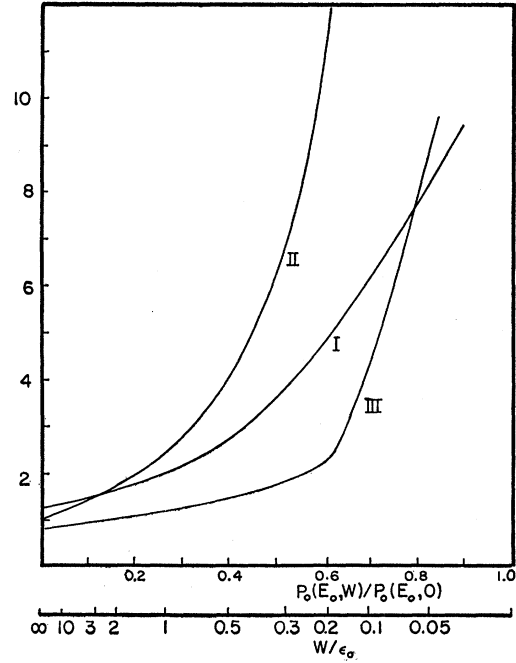| (W_1,W_2)	$(10,\infty)$	$(2,10)$	$(0.5,2)$	$(0.19,0.5)$
$\overline{W}_i$	20	3.75	0.92	0.31
$\sigma(\overline{W}_i)$	1.22	1.06	0.81	0.55

FIG. 7. Curve I: $g_0(E_0,W)/p_0(E_0,W)$. Curve II: $[\pi(E_0,W)/\Pi(E_0,0)]_{\text{Approx A}}/[p_0(E_0,W)/P_0(E_0,0)]$. Curve III: $1/\sigma(W)$. $\sigma(W)$ is a slowly varying function which ensures a correct normalization of the photon distribution functions for photon energies $W < 10\epsilon_0$ and is equal to [Curve I/Curve II].

(3) Transition Factors—$T(\overline{E}_i,\Delta E_j)$ and $T(\overline{W}_i,\Delta E_j)$

The calculations to be outlined in this section can be grouped into two portions. First, under the assumption that the secondary particles produced in the dural do not cause further multiplication we find transition factors which are labeled T_0. Second, the factors T_0 are used to obtain the transition factors T, which take account of the interactions of the secondaries. For example, we must find the numbers of photons in an energy range ΔW_j, which are radiated by electrons in any other possible energy range, of median energy $\overline{E}_i$, and which materialize before reaching the bottom of the dural layer. The inclusion of secondary interactions does not necessitate a revision of our general method as summarized in Eq. (6), since, for the example above, the electron pairs will be counted in the end as if they were created directly by the incident electrons.

The results of the first part of this work are shown in Table II. It is to be noted that though we calculate $T_0(\overline{E}_i,\Delta W_j)$, the number of photons in the energy range ΔW_j produced by electrons having a median energy $\overline{E}_i$ (so that their secondary electrons may be found), we do not present factors $T_0(\overline{W}_i,\Delta W_j)$ since processes in which photons are simply degraded in energy are not significant at these high energies.

The results of the second portion of the calculations are presented in Table III. By comparing the results of Tables II and III it is easily seen that the corrections for secondary interactions are small except at low

TABLE II. Transition factors T_0. Energies are in units of the critical energy ϵ_0.

ΔE_j or ΔW_j	$\bar{E}_i$ or $\bar{W}_i$			
	20	3.75	0.92	0.31
	$T_0(\bar{W}_i,\Delta E_j)$			
10–∞	0.207	0	0	0
2–10	0.158	0.172	0	0
0.5–2	0.036	0.144	0.160	0
0.19–0.5	0.007	0.034	0.101	0.112
0–0.19	0.004	0.013	0.051	0.130
	$T_0(\bar{E}_i,\Delta E_j)$			
10–∞	0.834	0	0	0
2–10	0.147	0.823	0	0
0.5–2	0.019	0.149	0.842	0
0.19–0.5	~0	0.019	0.122	0.831
0–0.19	~0	0.008	0.036	0.169
	$T_0(\bar{E}_i,\Delta W_j)$			
10–∞	0.168	0	0	0
2–10	0.490	0.141	0	0
0.5–2	0.495	0.402	0.115	0
0.19–0.5	0.342	0.341	0.262	0.068
0–0.19	0.607	0.588	0.555	0.393

energies, where, however, there are only a relatively small number of electrons. The treatment given the low-energy particles is straightforward and will be discussed briefly.

We neglect the incident electrons in the range $(0,0.19\epsilon_0)$ entirely, since it has been shown by Barker[27] that the average effective range of electrons of energy 16 Mev$=0.19\epsilon_0$ is 1.05-in. dural if ionization and radiation losses are fully taken into account. As we shall see below, the small numbers of incident photons in this energy range will scatter few electrons or produce few pairs of electrons having sufficient energy to penetrate the rest of the dural; and they have been neglected also. Thus, we must consider further only the low-energy secondaries produced in the dural.

It can easily be estimated that only about 20.2 percent of those electrons *produced* in the energy interval $(0,0.19\epsilon_0)$, by either pair production or radiation, from particles in higher energy ranges would be observed under the dural. It can also be shown that the number of observable electrons arising from Compton scattering of secondary photons in the energy range $(0.04\epsilon_0,0.19\epsilon_0)$ is about 3.3 percent of the number of photons, and almost independent of their energy, in this range. Since the probability of pair production is equal to the total probability for Compton scattering at about 16 Mev $=0.19\epsilon_0$, the Compton scattering factor has been doubled to give an approximate upper limit for both processes. The transition factors for these low-energy particles were then computed and listed in Table III.

The lateral distribution of electrons under 1.05-in. dural, $\mathfrak{N}(0,\infty;r)$, is then obtained, according to (7), by multiplying each lateral distribution curve found in Secs. III.A(1) and III.A(2) by the sum of the appropriate transition factors from Table III and adding. The result is shown in Fig. 6.

[27] P. R. Barker, thesis, University of Michigan, 1952 (unpublished).

B. Ionization Chamber Response Curves

A set of curves has been prepared which gives the number of shower electrons passing through the sensitive volume of each wire when showers characterized by a lateral distribution function $\mathfrak{N}(0,\infty;r)$ pass through the plane of observation in the vicinity of the chamber. The coordinates in the plane of observation have been designated "wire number" and δ. The ion-chamber wires are labeled with consecutive integers from the shower axis outward. δ is the distance of the shower core from the center of the chamber in a direction perpendicular to the long axis of the chamber (see Fig. 2). This set of response curves is shown in Fig. 8 and assumes a total number of electrons $\Pi(E_0,0,t) = 2 \times 10^4$. Since the number of electrons N_i per channel is directly proportional to Π, curves for different values of Π are easily obtained from those of Fig. 8.

In general, Fig. 8 presents 2 curves for every value of δ, though the curves differ only near the shower axis. Each peaked curve is for a shower that hits one wire (numbered 0) directly. Each flat-topped curve is for a shower which hits between 2 wires. The dotted curve shows the response of the chamber, for $\delta=0$, to a Molière distribution, which is not corrected for the transition effect. If all ordinates of this response curve are multiplied by a factor 2, then the curve is almost identical to the response curve, corrected for the transition effect, for $\delta=23.5$ cm. We see that the transition effect sharpens the distribution by increasing the peak height and decreasing the half-width slightly. This is to be expected since: (1) the spread of a shower is proportional to the characteristic scattering length, which is 80 m for air and 4 cm for Al; and (2) the multiplication of the high-energy particles is inversely proportional to the radiation length, which is 37.7 g/cm² for air and 24.5 g/cm² for Al, while the energy loss by collision for the low-energy electrons per g/cm² is almost the same for air and aluminum.

C. Systematic Departures from the Response Curves

The response curves were obtained under the assumption of a lateral distribution function for a cascade shower, initiated by one particle and observed at its maximum. Thus, it would be expected that the experi-

TABLE III. Transition factors $T(\bar{E}_i,\Delta E_j)$ and $T(\bar{W}_i,\Delta E_j)$. Energies are in units of the critical energy ϵ_0.

ΔE_j	$\bar{E}_i$				$\bar{W}_i$			
	20	3.75	0.92	0.31	20	3.75	0.92	0.31
10–∞	0.85	0	0	0	0.19	0	0	0
2–10	0.19	0.83	0	0	0.17	0.16	0	0
0.5–2	0.11	0.18	0.85	0	0.06	0.15	0.15	0
0.19–0.5	0.05	0.06	0.12	0.83	0.02	0.05	0.10	0.10
0–0.19	0.06	0.05	0.05	0.06	0.01	0.01	0.02	0.03
	$\Sigma_j\, T(\bar{E}_i,\Delta E_j)$				$\Sigma_j\, T(\bar{W}_i,\Delta E_j)$			
0–∞	1.26	1.12	1.02	0.89	0.45	0.37	0.27	0.13

mental data will exhibit systematic departures from the theoretical curves.

First, if one considers the region around the shower axis where the majority of all electrons have energies $E \gg \epsilon_0$, that is, $r \ll r_1$, it has been shown[28] that the total distribution function has a singularity which behaves as $1/r^{2-s}$ where, of course, $s=1$ for the shower maximum. Though it would be difficult to ascertain the exact effect which would result from our attempt to analyze data from relatively old showers on the basis of curves calculated for the shower maximum, it is plausible that, if δ may be used as a variable parameter, the distribution in the assigned values of δ would not be random; i.e., there would be no events which fit the response curve for $\delta=0$, but there would be a disproportinate number which fit the curves for rather large values of δ.

Second, it is to be expected as discussed in Sec. I that the large air showers are, in general, superpositions of showers of various energies initiated by decay photons from more than one π^0 meson. In order to be able to resolve multiple maxima in this experiment, the separate showers giving rise to the individual maxima must have (1) comparable energies, (2) separations $d \gtrsim 30$ cm, and (3) their cores lying on a line nearly parallel to the long axis of the ion chamber. With these requirements in mind, we shall consider single and multiple π^0 production.

If a single π^0 meson is the precursor of a shower, a double core would be expected. In order to ascertain whether or not the structure should be observed experimentally, the energies and angular separations of the decay photons must be determined. In the extreme relativistic case, $E_{\pi^0} \gg m_0 c^2$, where E_{π^0} is the energy of the meson and m_0 its rest mass, it can easily be shown that to a very good approximation the angular separation is $2m_0 c^2/E_{\pi^0}$. The approximation becomes poor only when most of the energy of the π^0 is carried off by one of the photons. However, the resulting shower structure would not be resolvable under this condition because of statistics. If the neutral mesons are assumed to have been produced at an altitude of 15 km, the above expression implies a lateral separation of π^0-decay-photon showers of

$$d(\text{cm}) = 4.1 \times 10^{14}/E_{\pi^0}(\text{ev}).$$

The question of the separations to be expected between cores produced by two or more neutral mesons is, probably, still unanswered. The suggestion of Lewis et al.[1] is not satisfying because, contrary to experiment, it predicts multiplicities of about 100 at the usual shower energies with core separations of about 10 meters at the observation level. By using the thermodynamic approximation[29] of Fermi's statistical theory of multiple

[28] I. Pomeranchuk, J. Phys. (U.S.S.R.) 8, 17 (1944); A. Migdal, J. Phys. (U.S.S.R.) 9, 183 (1945); J. Nishimura and K. Kamata, Progr. Theoret. Phys. (Japan) 5, 899 (1950).
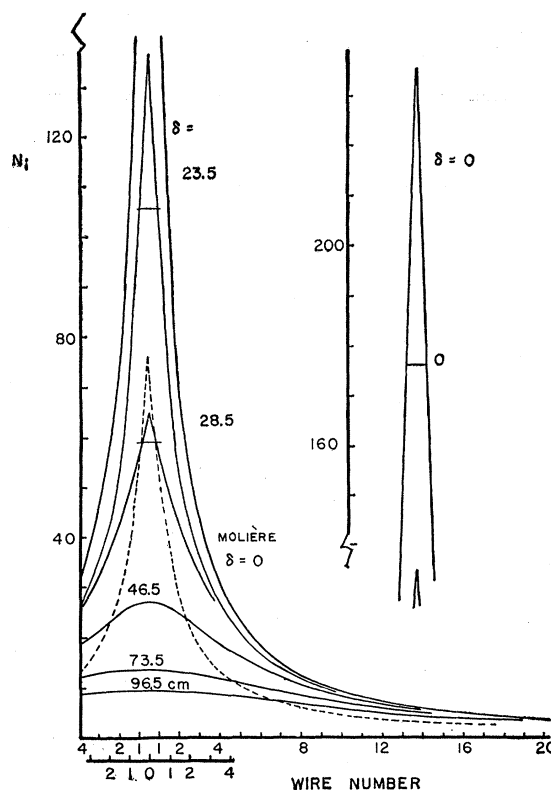[29] E. Fermi, Phys. Rev. 81, 683 (1951).

FIG. 8. Chamber response curves: the number of electrons N_i passing through the sensitive volume of wire number i when the axis of a shower containing $\Pi = 2 \times 10^4$ electrons passes through the plane of observation at a perpendicular distance δ from the long axis of the chamber. The dotted curve is the response assuming a Molière distribution uncorrected for the transition effect in the dural above the chamber volume.

meson production, estimates closer to experimental observations have been obtained.[7] The predicted separations are still too large—about 1 to 10 meters—to be in agreement with shower data.

The possible roles which the highly interacting N component of the showers may play in the production of a soft component related only indirectly to the showers produced in the initial primary interaction have not been discussed so far. A quantitative estimate of its contribution to the electronic distribution function is impossible at present. It can be expected, however, that a general background of lower-energy showers is added to the initial shower, or showers. The low energy is a result of the degradation of the energy reaching the soft component via the nucleonic cascade.

D. Fluctuations

A given density distribution found in the ion chamber may be interpreted adequately only if the fluctuations in the lateral distribution function are known or can be estimated. Blatt[23] has concluded in a qualitative way that the fluctuations should not be much larger than those expected if the shower particles are completely

TABLE IV. Numbers of fluctuation cores of various energies found at distances r from the shower axis between r_1 and r_2 which result from single, large-angle scattering of high-energy electrons early in the shower development.

$t(X_0)$	h(km)	Π	E	$N(r_1,r_2)$	E_0 10^{13} ev r_1	r_2	10^{14} ev r_1	r_2(cm)
1	13	2	$E_0/2$	<0.009	17	34	1.7	3.4
				0.035	8	17	0.8	1.7
				0.139	4	8	0.4	0.8
2	12	2	$E_0/4$	<0.009	31	62	3.1	6.2
				0.035	15	31	1.5	3.1
				0.139	8	15	0.8	1.5
3	10.8	6	$E_0/8$	<0.027	56	112	5.6	11.2
				0.105	28	56	2.8	5.6
				0.41	14	28	1.4	2.8
				1.7	7	14	0.7	1.4
4	10	10	$E_0/16$	<0.044	100	200	10	20
				0.174	50	100	5	10
				0.695	25	50	2.5	5.0
				2.8	12.5	25	1.25	2.5
5	9	22	$E_0/32$	<0.10	180	360	18	36
				0.38	90	180	9.0	18.0
				1.53	40	90	4.0	9.0
				6.2	20	40	2.0	4.0

independent. For our experiment this implies that the fluctuations in the response of each detector area would be $\sqrt{\bar{N}_i}$, where $\bar{N}_i$ is the average number of electrons passing through the ith area.

As Blatt points out, the fluctuations in the lateral distribution feature (1) a "short memory" and (2) a "small amplification." The short memory is a result of the large displacement (>>10 cm, the wire spacing of our chamber) of electrons from their point of origin caused by multiple scattering when their energy is low enough for them to be found an appreciable distance (many wire spacings in this experiment) from the shower axis. If their energy is this low, then these electrons produce few secondaries and show a small amplification for fluctuations. Illustrative examples of the above statements are readily obtained by picking an energy for the electrons, finding their rms displacement from the shower axis, and calculating their rms displacement per radiation length due to multiple scattering. It is then seen that the electrons must have an energy $\gg\epsilon_0$ in order for their progeny to appear to be related in their lateral position. Since we shall have a detailed view of the structure near the shower axis in this experiment, it is necessary to consider the possible consequences of fluctuations of the very high-energy electrons found near the shower axis. We shall therefore calculate the probability that one of the high-energy electrons found in the early development of the shower undergoes a single, large angle scattering, so that its progeny resembles an auxiliary shower having an independent origin.

Since a model of the shower development is required, we assume that a photon of energy E_0, produced 3

radiation lengths ($\gtrsim 125$ g/cm^2) down from the top of the atmosphere, initiates a shower in which each electron and photon produces two equally energetic particles by radiative and pair production processes, respectively, for each radiation length of air traversed. Table IV is a collection of the numbers which have been obtained[17] from this model for two initiating energies. Π is the total number of electrons at depth t, and E is their energy. The numbers of such cores $N(r_1,r_2)$ found at a distance r between r_1 and r_2 from the main shower axis are negligibly different if primary electrons are assumed.

As an example, it is seen that in 3.5 percent of the cases of 10^{13}-ev showers, two equally energetic "fluctuation cores" (as these fluctuations will be called) of energy 5×10^{12} are found separated by distances of from 8 to 17 cm, with the majority having the smaller separation $(N \sim 1/r^3)$. An upper limit of 0.9 percent have separations of from 17 to 34 cm. For comparison, the most probable separation for two π^0 decay-photon showers at this energy is 41 cm. It is also seen that, for this experiment, fluctuations of this type are negligible for energies $E_0 \gtrsim 10^{14}$ ev.

From the above discussion it appears justifiable to assume that, except in the rare case in which a fluctuation core is found, the rms fluctuations in the numbers of electrons per channel in the chamber are only negligibly larger than $\sqrt{N_i}$. Actually, since there is a spacial dependency introduced in the positions of the pairs of electrons produced in the materialization of photons in the dural, the transition effect increases the fluctuations to about $2\sqrt{N_i}/\sqrt{3} = 1.15\sqrt{N_i}$.
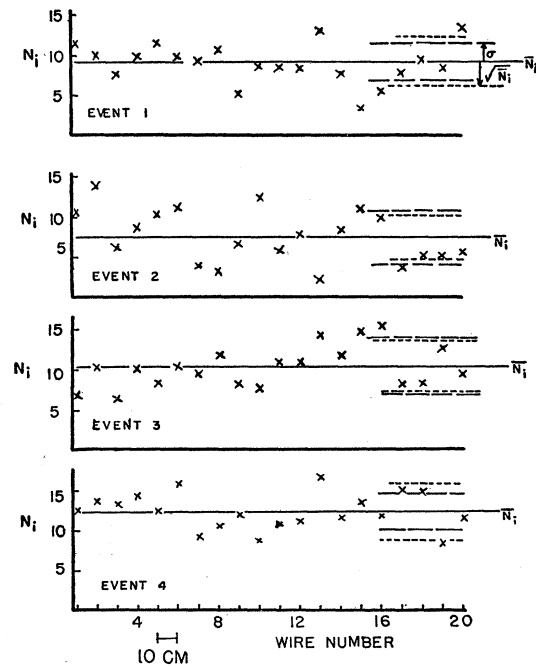

FIG. 9. Events showing a flat distribution of ionization and no systematic fluctuations.
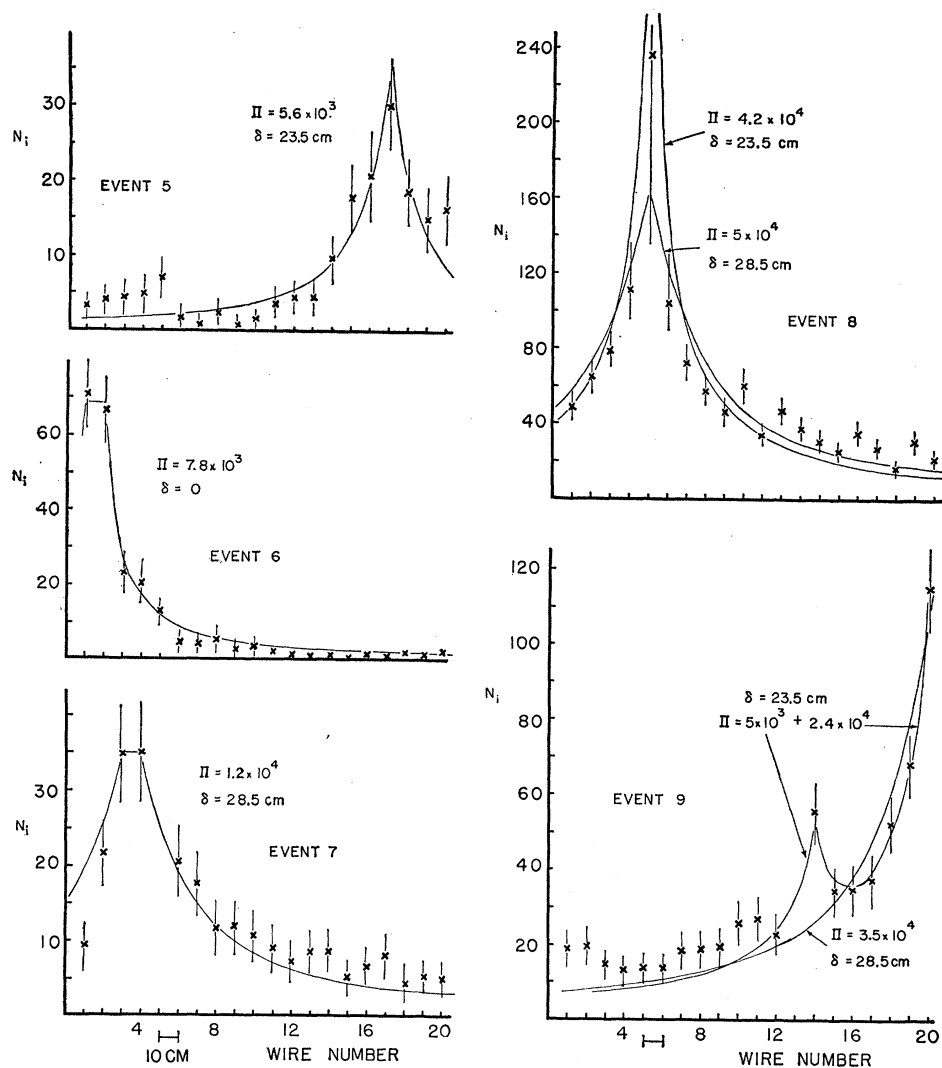
FIG. 10. Events showing marked changes in electron density over the length of the chamber.

IV. EXPERIMENTAL RESULTS

A. Individual Events

The four-fold coincidence rate of the Geiger counter arrangement described in II was 4.10 ± 0.13 hr^{-1}; in a total running time of 109 hours about 430 shower events were recorded. The reduced data for the most interesting events are shown in Figs. 9–12. In plotting these results the wires have been numbered consecutively from one end of the chamber and the number of electrons passing through the sensitive volume of wire i is denoted by N_i. In almost every case the indicated errors are $1.15\sqrt{N_i}$.

The first group, events 1–4, showed no systematic change in density over the chamber and were selected because they were the largest of their type observed. They are assumed to be caused by high-energy showers whose axes pass through the plane of observation relatively far from the chamber. The close agreement

between $\sqrt{N_i}$ and σ, the rms deviation from the mean, show that at least far from the shower axis the fluctuations are not larger than expected.

The second group, events 5–9, exhibit rather striking changes in density over the chamber, and have been interpreted to be the result of showers whose axes passed through the chamber area or were immediately adjacent thereto. Response curves from Fig. 8 have been selected which can perhaps best represent the data and are shown on the figures. In general, the agreement is not too unsatisfactory and appears to require no drastic revision of the lateral distribution function calculated in III. In event 6 a shower core was assumed to have passed between the first two wires of the chamber since N_1 and N_2, the numbers of electrons passing through the first and second detector areas, were so nearly equal while the ratio N_2/N_3 is so very large. Event 8 was the largest obtained, and the height of the peak has not been determined very
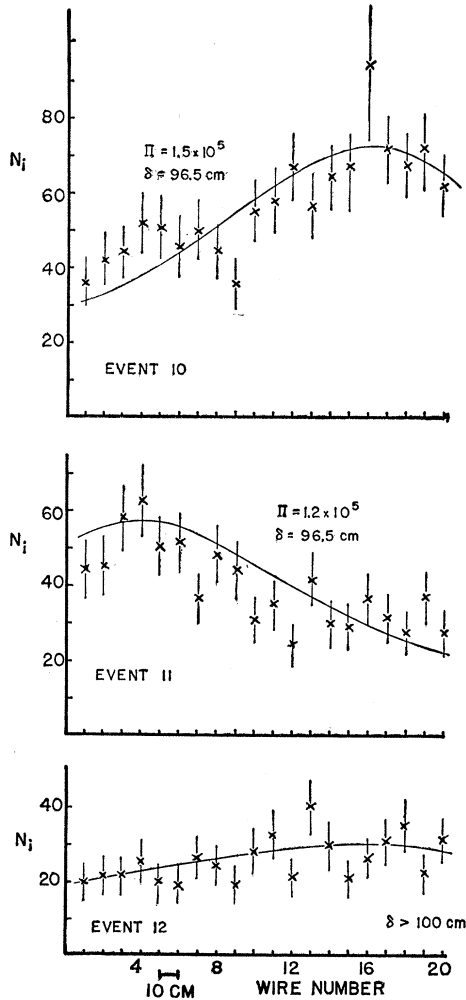
FIG. 11. Events which exhibit small, but consistent, changes in electron density across the length of the chamber.

accurately since the center channel was overloaded and its response could only be estimated by the amount of undershoot. The two immediately adjacent channels were just at the overload level. Therefore, two curves have been chosen, but they show too little difference to make a choice between them readily apparent. The attempt to fit event 9 with a single response curve from Fig. 8 is less satisfactory than for the other events in this group. Adding an auxiliary shower whose core hits wire No. 14 gives a better fit over the region nearest the main core, but does not provide any improvement in fitting the tail. By fitting events 8 and 9 with a single shower curve it has been necessary to make a compromise between picking a response curve which had a half-width narrow enough (δ small) and a tail which was high enough (δ large).

The next three events, 10–12, have been ascribed to showers whose axes hit relatively too far from the chamber area to show a very pronounced maximum.

For the showers shown here, the statistics are too poor to rule out fits using monotonically increasing or decreasing response curves. There is relatively poor agreement between the data and the curve shown for event 11.

Though the last two events shown, 13 and 14, have relatively flat distributions, they have fluctuations from the average which are almost twice $1.15\sqrt{\bar{N}_i}$ and which show a systematic behavior across the chamber. The former event is difficult to interpret except in terms of two separate shower axes, presumably due to π^0 mesons. Event 14 is particularly difficult because more than two response curves must be utilized to obtain very much better agreement than that obtained using only one slowly varying curve.

B. Discussion and Conclusions

The events which have been studied in detail were selected individually from the events recorded either on the basis of significant changes in density over the length of the chamber or on the basis of a large density of particles regardless of their distribution. The triggering system would, of course, tend to introduce such a selection already, but introduces no serious bias. The coincidence rate is about 16 percent higher than that found by Cocconi et al.[30] at sea level, but can be explained by the somewhat closer counter spacing used here. The effect of the $\frac{1}{4}$-in. Pb shielding on the counters is difficult to assess because the transition effect has been shown in III to depend upon distance from the shower axis.
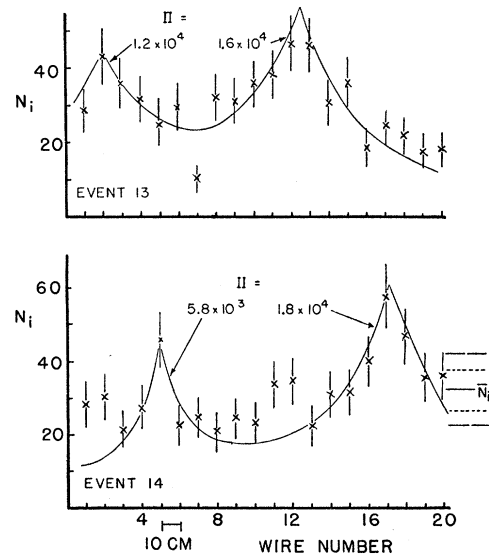

FIG. 12. Events which show electron density distributions which are (a) unlike those expected from single showers whose axes pass through or close by the chamber and (b) difficult to attribute to showers whose axes pass far from the chamber because of the large, systematic fluctuations observed in the chamber response.

[30] Cocconi, Tongiorgi, and Greisen, Phys. Rev. 75, 1063 (1949).

Since the showers observed here would be quite far beyond their maximum if they were initiated about one mean free path (for nuclear interaction of the cosmic-ray N-component) down in the atmosphere, it is perhaps surprising to find electron density distributions which are as sharp as those of events 5–9. This is especially true since previous experiments[8,13] at mountain altitudes have indicated that the showers found there are less peaked within about one meter of the shower axis than predicted by the Molière distribution. A reconciliation can be made if event 6 is attributed to either a very young shower or a few highly ionizing rays emerging from the dural lid of the chamber. Then, the curves fitted to the other 4 events in the chamber have values of δ which are about equal to the half width of the chamber. Such a distribution in δ values implies a structure function flatter than that assumed. On the other hand, it was found that for the two largest events, 8 and 9, that the half-width was too small compared to the height of the tails for a good fit with our theoretical curves. It is possible that the transition effect in the high-energy core of older showers differs strongly from that for showers at their maximum. It is also possible that a large number of widely scattered small showers created by the N-component cascade could account for the high density found in the tails. Though there appear to be several large fluctuations in the tails of events 8 and 9 which tend to support the latter possibility, it is not profitable to pursue either of the above alternative explanations on the basis of the data presented here.

An attempt to attribute the auxiliary shower drawn in event 9 to either a π^0-decay photon or a fluctuation core associated with the main shower fails completely. By referring to Sec. III.C., it can be shown that if a π^0 meson of energy 2×10^{13} ev decays into photons of $\frac{1}{4}E_{\pi^0}$ and $\frac{3}{4}E_{\pi^0}$, then a multiple curve which exactly fits the response of wires numbered 6–19 in event 5 would be obtained. Since the statistics are too poor in this event to distinguish such structure, and since for higher energy π^0's the core separations would be even smaller than 20 cm, it can be seen that π^0-decay photon showers would not be resolved with this apparatus. By referring to Sec. III.D., it can be shown that the structure discussed above for event 5 would occur in only 2 out of 100 cases because of "fluctuation cores."

The last two events, 13 and 14, appear to be the profiles of showers which have been described[13] recently in the literature as "lumpy." The percentage of such cases found in this experiment (2 out of 7) corresponds roughly to that found in reference 13 (8 out of 39), though these figures are probably quite dependent upon the methods of selection used. Since it is difficult to accept the conclusion that the systematic deviations in the chamber response found in these events are caused by fluctuations in the lateral structure of a single shower, these events are attributed to cascade showers initiated by at least two particles having comparable energies.